Observation of strong electromagnetic fields around laser-entrance holes of ignition-scale hohlraums in inertial-confinement fusion experiments at the National Ignition Facility

2013 New J. Phys. 15 025040

(http://iopscience.iop.org/1367-2630/15/2/025040)

New Journal of Physics
The open access journal for physics

Observation of strong electromagnetic fields around laser-entrance holes of ignition-scale hohlraums in inertial-confinement fusion experiments at the National Ignition Facility

C K Li[1,4], A B Zylstra[1], J A Frenje[1], F H Séguin[1], N Sinenian[1], R D Petrasso[1], P A Amendt[2], R Bionta[2], S Friedrich[2], G W Collins[2], E Dewald[2], T Döppner[2], S H Glenzer[2], D G Hicks[2], O L Landen[2], J D Kilkenny[2], A J Mackinnon[2], N Meezan[2], J Ralph[2], J R Rygg[2], J Kline[3] and G Kyrala[3]

[1] Plasma Science and Fusion Center, Massachusetts Institute of Technology, Cambridge, MA 02139 USA
[2] Lawrence Livermore National Laboratory, Livermore, CA 94550 USA
[3] Los Alamos National Laboratory, Los Alamos, NM 87545 USA
E-mail: ckli@MIT.edu

New Journal of Physics **15** (2013) 025040 (14pp)
Received 20 July 2012
Published 27 February 2013
Online at http://www.njp.org/
doi:10.1088/1367-2630/15/2/025040

Abstract. Energy spectra and spectrally resolved one-dimensional fluence images of self-emitted charged-fusion products (14.7 MeV D^3He protons) are routinely measured from indirectly driven inertial-confinement fusion (ICF) experiments utilizing ignition-scaled hohlraums at the National Ignition Facility (NIF). A striking and consistent feature of these images is that the fluence of protons leaving the ICF target in the direction of the hohlraum's laser entrance holes (LEHs) is very nonuniform spatially, in contrast to the very uniform fluence of protons leaving through the hohlraum equator. In addition, the measured nonuniformities are unpredictable, and vary greatly from shot to shot. These

[4] Author to whom any correspondence should be addressed.

observations were made separately at the times of shock flash and of compression burn, indicating that the asymmetry persists even at ∼0.5–2.5 ns after the laser has turned off. These phenomena have also been observed in experiments on the OMEGA laser facility with energy-scaled hohlraums, suggesting that the underlying physics is similar. Comprehensive data sets provide compelling evidence that the nonuniformities result from proton deflections due to strong spontaneous electromagnetic fields around the hohlraum LEHs. Although it has not yet been possible to uniquely determine whether the fields are magnetic (B) or electric (E), preliminary analysis indicates that the strength is ∼1 MG if B fields or $\sim 10^9$ V cm^{-1} if E fields. These measurements provide important physics insight into the ongoing ignition experiments at the NIF. Understanding the generation, evolution, interaction and dissipation of the self-generated fields may help to answer many physics questions, such as why the electron temperatures measured in the LEH region are anomalously large, and may help to validate hydrodynamic models of plasma dynamics prior to plasma stagnation in the center of the hohlraum.

Contents

1. Introduction **2**
2. Experimental results **3**
3. Data characteristics **8**
3.1. Unpredictable spatial but repeatable temporal occurrences 8
3.2. Scale of spatial nonuniformity 8
3.3. Undistinguishable field types 9
3.4. Estimate of field strengths 11
4. Similar observations from OMEGA experiments **11**
5. Summary **13**
Acknowledgments **13**
References **13**

1. Introduction

The goal of inertial-confinement fusion (ICF) is to achieve fusion ignition and high energy gain [1–4], which requires that a cryogenic deuterium–tritium (DT) spherical capsule be symmetrically imploded. The implosion results in a small mass of low-density, hot fuel at the center, surrounded by a larger mass of high-density, low-temperature main fuel [2–4]. Such an exciting scientific breakthrough is being vigorously pursued at the National Ignition Facility (NIF) [5] through the indirect-drive approach, in which the capsule implosion occurs in response to tremendous radiation pressure generated by the thermal x-rays in a high-Z enclosure, i.e. hohlraum, when the enclosure's inner wall is irradiated by high-power lasers [5–20]. The lasers would have a temporal pulse shape designed to launch four radially convergent shock waves which would coalesce at the capsule center, creating a self-igniting 'hot spot' which would generate a self-sustaining burn wave that propagates into the main fuel region.

The National Ignition Campaign (NIC) aims to eventually realize this important goal at the NIF, which has unique capabilities including 192 laser beams and 1.8 MJ of 3ω (0.35 μm) laser energy, enhanced pulse-shaping capabilities and pulse durations and greatly improved irradiation symmetry, etc [5–20]. Several ongoing experimental campaigns have been conducted to tune implosion conditions and to address a wide range of critical physics issues relevant to ignition sciences, including laser coupling, implosion dynamics and symmetry, hot spot formation and burn physics, etc. Many of these campaigns use D^3He gas-filled capsules as surrogates for cryogenic DT layered targets, and these implosions produce the fusion reaction $D + {}^3He \rightarrow \alpha + p$ (14.7 MeV).

In this paper, we discuss spatial and spectral measurements [21] of self-emitted charged particles (14.7 MeV D^3He protons) from NIF indirect-drive ICF implosions, made simultaneously on particles leaving through laser entrance holes (LEHs) and particles leaving through the hohlraum equator. As we will see in section 2, data from recent NIC experiments have consistently demonstrated large nonuniformities in the fluence of self-emitted charged fusion products that leave capsules in ignition-scale hohlraums through the LEHs, providing compelling evidence of self-generated electromagnetic fields appearing around the LEHs. Such nonuniformities are not seen in particles leaving the hohlraums in the equatorial direction. Issues of significant interest include proton deflection patterns and spatial distributions; field types (E or B) and strengths; mechanisms of field generation; and field effects and implications, as discussed in section 3. To further explore the underlying physics and mechanisms behind field generation in hohlraums, additional information from indirect-drive experiments at the OMEGA laser facility [22] is also presented in section 4. Section 5 summarizes the work.

These observations have motivated significant interest in how such fields affect hohlraum plasma dynamics. In particular, the effects of fields on the distributions and evolution of plasma electron temperature (T_e) and density (n_e) are of critical importance because they could affect the electron thermal transport, seed laser–plasma instabilities and distort the drive uniformity. In addition, understanding the generation, evolution, interaction and dissipation of these fields may help to explain the large T_e measured in the LEH region and its spatial structure and dynamics, and to validate the hydrodynamic models prior to stagnation in the center of the hohlraum.

2. Experimental results

The experiments performed at the NIF are illustrated schematically in figures 1 and 2. The hohlraums were of the typical ignition-scale size with 5.44 mm diameter, 10.0 mm length and LEHs with 3.48 mm diameter, as shown in figure 1. The hohlraum wall consisted typically of 34 μm Au and 74 μm Al (overcoated externally on the Au). The capsule inside a hohlraum was a warm plastic (CH) one with ~2 mm diameter and filled with D^3He gas. Each hohlraum was driven by 192 laser beams forming four single irradiation rings, with total laser energy of ~1–1.5 MJ in a typical [6–20] four-shock pulse (lasting ~14.9–19.9 ns). The individual laser beams had full spatial and temporal smoothing [5–20].

As shown in figure 2, self-emitted 14.7 MeV D^3He fusion protons were recorded by a number of wedge-range filter (WRF) proton spectrometers [23, 24]. Two were placed on port DIM (0, 0) to probe protons emitted from the hohlraum LEH (pole direction), and another two were placed on DIM (90, 78) to probe protons emitted from the hohlraum equator, as shown in figure 1 and discussed in [21]. The active surface of each WRF is about $2.4 \times 2.4\,cm^2$, subtending an angle of ~2.7° at the capsule; thus it sampled a plasma area of $\sim 0.2 \times 0.2\,mm^2$

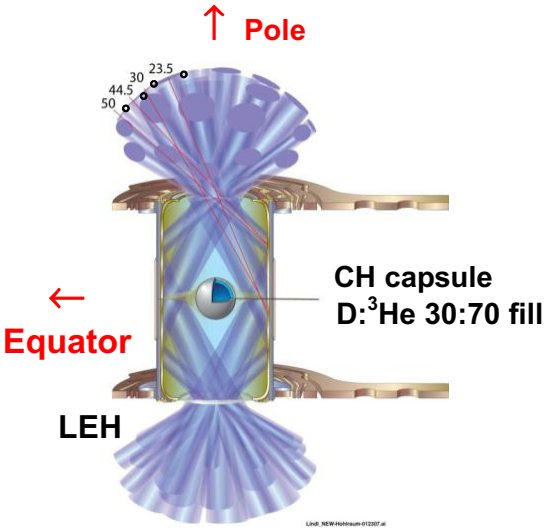

Figure 1. Schematic illustration of the NIF hohlraum structure and laser beam arrangements for these experiments. The typical hohlraum is about 5.44 mm in diameter and 10 mm long, and has walls consisting of 34 μm Au and 74 μm Al (overcoated on the Au). As indicated in figure 2, self-emitted protons from the capsule are observed with spectrometers in both the pole (LEH) and equator directions.

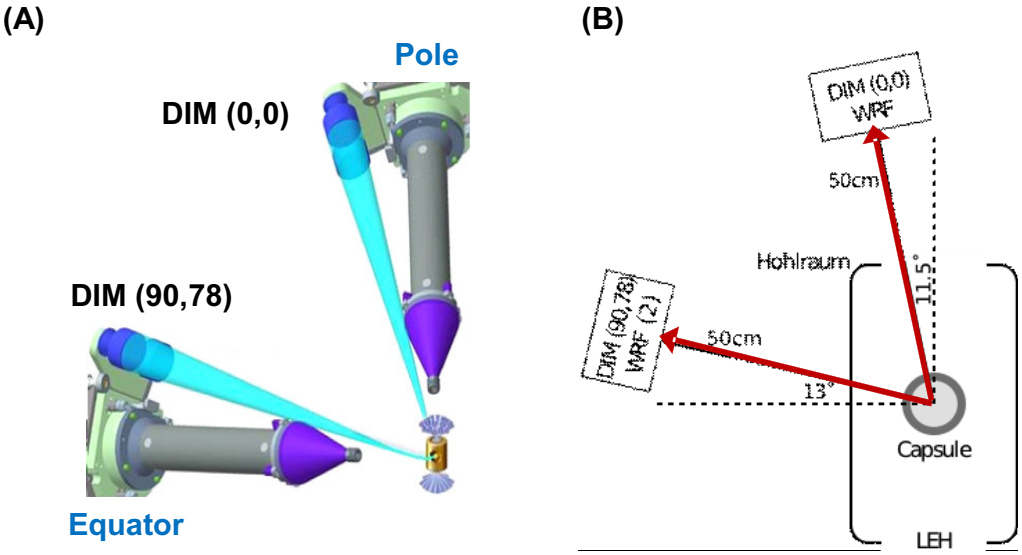

Figure 2. Experimental setup for a typical NIC shot (A). Four WRF proton spectrometers were placed on the GXD holders; two of them were on DIM (0, 0) to probe charged particles emitted through the hohlraum LEH and another two were placed on DIM (90, 78) to probe charged particles emitted from the equator (B).

at the LEH or $\sim 0.1 \times 0.1\,\mathrm{mm}^2$ near the equatorial hohlraum wall. Measuring the number and energy spectra of fusion charged-particle products provides important information about fusion yields, fuel and shell temperatures, areal densities, implosion symmetry and dynamics,

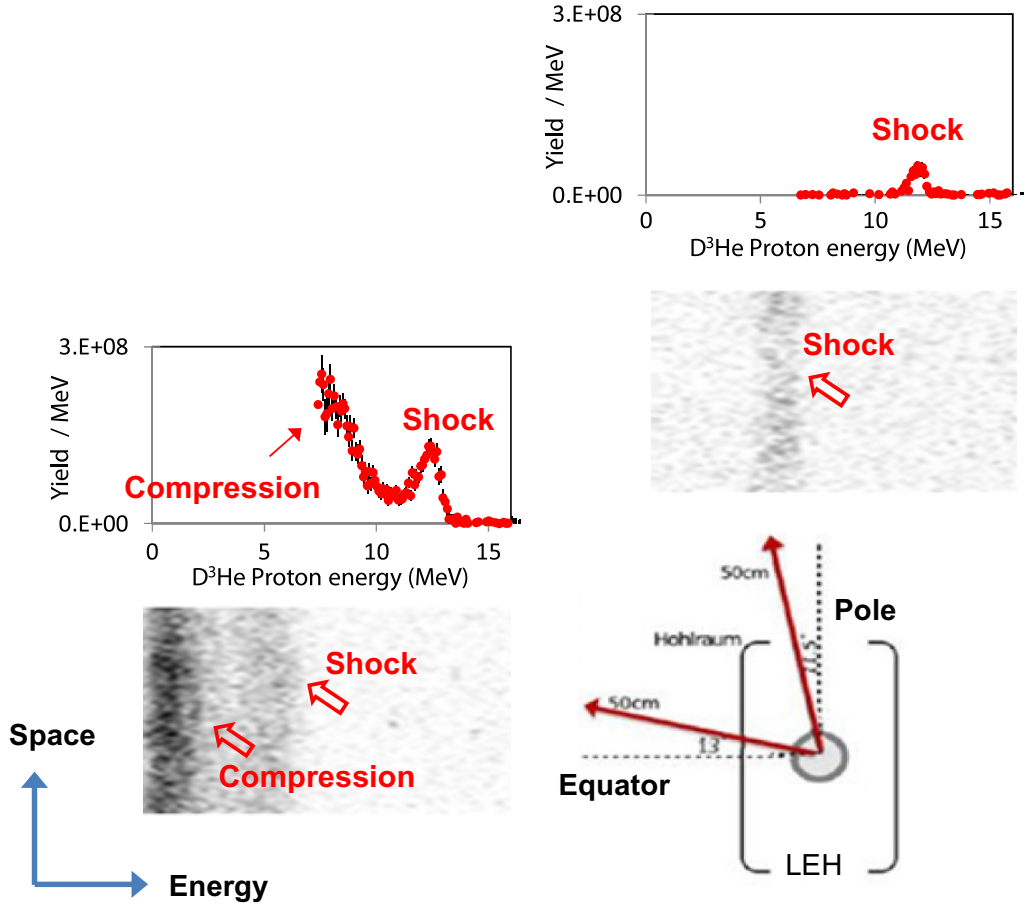

Figure 3. Typical images of proton fluence as a function of energy and spatial direction of self-emitted protons generated from the fusion reaction of D and ^{3}He in an indirect-drive, NIC ICF implosion (shot N101211). Data were acquired simultaneously at two different angles. The high-energy peak in each spectrum is associated with shock-flash burn, and the low-energy part seen in the equatorial direction results from compression burn. (Note that the equatorial spectrum above has been corrected for the extra energy lost by the protons while passing through the hohlraum wall.)

and fields, allowing us to characterize and quantify the hohlraum conditions and implosion performance in these experiments.

Figure 3 shows the nature of the proton data that were recorded. Each WRF spectrometer can provide a spectrally resolved one-dimensional image in which one direction (shown horizontal in the figures) represents energy and the other represents one spatial direction. Thus a horizontal lineout made in a small part of the 'space' range represents the proton spectrum at that spatial position, while a horizontal lineout in a different part of the 'space' range represents the spectrum at a different physical position. In this case (NIF implosion N101211) the D^{3}He protons were produced during the nuclear burn in implosion N101211. Note that the equatorial spectrum has been corrected for the extra energy lost by the protons while passing through the hohlraum wall, using information from the program SRIM [25] (see figure 4) and confirmed with calculations with the two-dimensional (2D) code HYDRA.

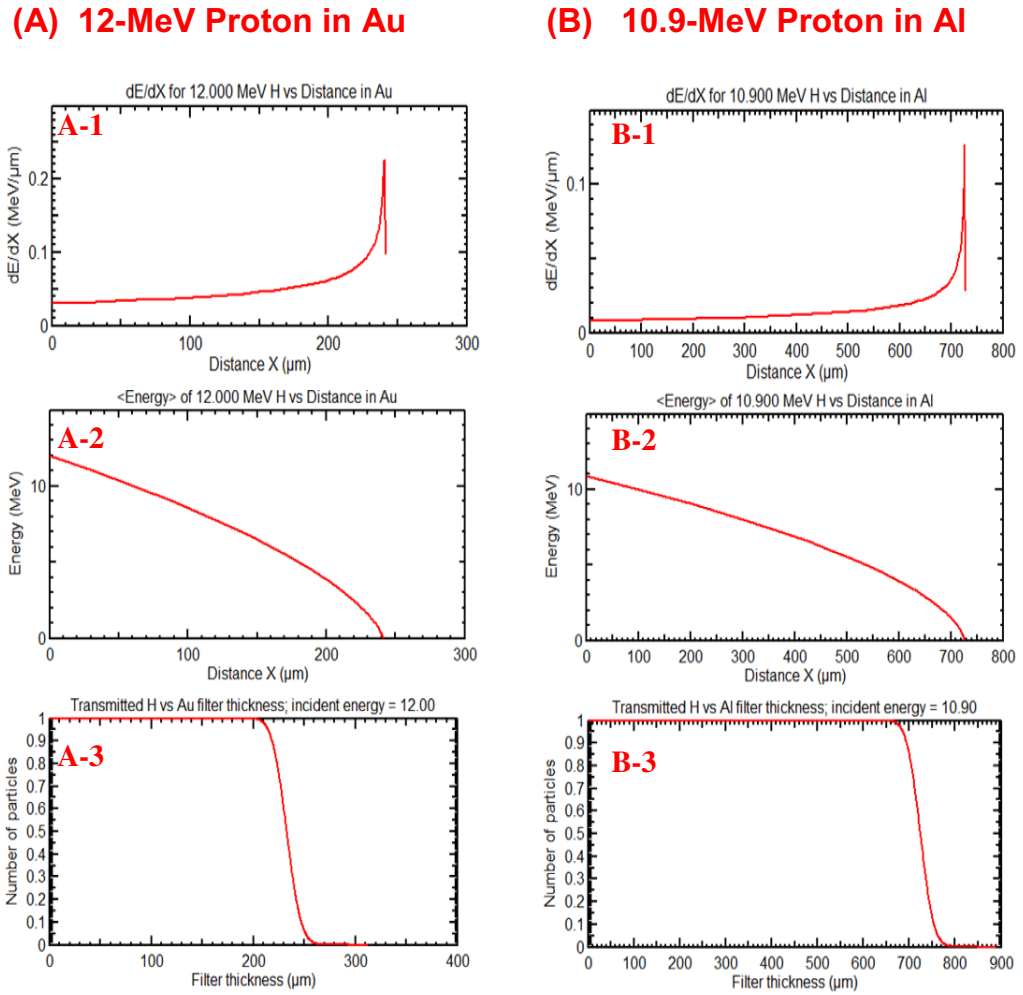

Figure 4. Calculated stopping power, energy loss and transmission of 12 MeV (10.9 MeV) protons as a function of travel distance in Au (Al) material are shown in (A) and (B).

Fusion protons were generated at two different times (∼700 ps separation for this shot): after shock convergence at the center of the imploded core (shock flash) and later when fuel burn occurs near the capsule peak compression (compression burn). The WRF data are time integrated, but the proton yields associated with both shock-flash burn and compression burn are seen separately because they occur at different energies. Both features are prominent in the equatorial data, while only a small fraction of shock-flash burn and virtually none of the compression burn was measured in the direction of the hohlraum LEH.

Such a difference between fluence uniformity in the equatorial and polar directions is repeatedly observed in virtually all implosions. Sometimes differences in the shock yield are even seen between two adjacent spectrometers. To study this, we placed two detectors with 7 cm center-to-center separation in the polar direction DIM (0, 0) and two more in the equatorial DIM (90, 78). In each direction, the two detectors are henceforth labeled 'Position 1' and 'Position 2'. Figure 5 shows that while the proton fluence in the direction of the equator is spatially uniform, the fluence is nonuniform in the direction of the LEH. In particular,

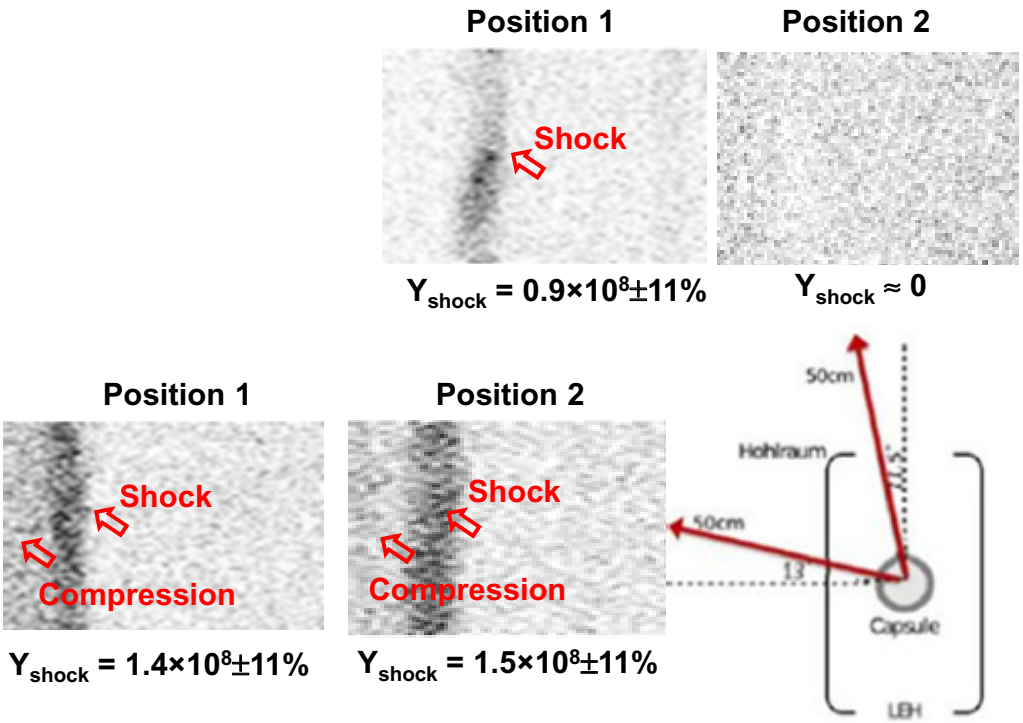

Figure 5. Typical images of self-emitted D^3He-proton fluence versus energy and space, in an indirect-drive NIC ICF implosion (shot N101220), acquired simultaneously at two different angles. The high-energy peak in each spectrum is associated with shock-flash burn (Y_{shock} is the D^3He fusion yield during the time of shock flash), and the low-energy parts in the equatorial images result from compression burn.

in the direction of the LEH although shock-flash protons were detected at Position 1, with some nonuniformity in the spatial direction, virtually no shock-flash protons were recorded at Position 2. This indicates that fluence nonuniformities were observed not only within a single detector, but also between two adjacent detectors, and the latter seems to approximately give a maximum angle of deflection that we are able to measure currently and therefore provides a lower limit of the deflection in this direction.

These fluence nonuniformities do not indicate that the implosions are asymmetric, but rather suggest the existence of self-generated fields around the LEHs at both shock-flash and compression-burn times. We can rule out angular variations in capsule areal density (ρR) as sources of the proton nonuniformity in the LEH direction. Qualitatively, the argument is that large variations in fluence due to ρR nonuniformity would require large differences in the amount of scattering for particles passing through regions with different ρR, but that would lead to large differences in energy [26], which we do not see. This was described and demonstrated quantitatively (with Monte-Carlo simulations) in [27], for direct-drive experiments that had capsules with similar ρR and that also had proton nonuniformities, leading to the conclusion that fields were present there. In addition, we will see in related experiments described below (figure 9) that when a large local enhancement in fluence is seen it is not associated with a measurable change in proton energy. Consequently, the observed nonuniformities indicate that

the existence of strong fields around the LEHs at the times of shock flash and compression deflected the protons without changing their energies. Furthermore, in this shot the laser beams were turned off at ∼19.8 ns, and x-ray bang time (the time of peak x-ray emission from the capsule central region) was $t \sim 21.42 \pm 0.07$ ns. Consequently, data on N101022 strongly indicate the existence of fields in the region of LEH even 1–1.5 ns after the laser beams were turned off.

3. Data characteristics

Several striking features have been identified in the measurements presented above. These data can be further used to quantitatively interpret the fluence nonuniformities seen in the LEH direction and their relationship to fields. It is important for us to understand the mechanisms of the field generation and evolution, and their effects on hohlraum dynamics.

3.1. Unpredictable spatial but repeatable temporal occurrences

Figure 6 shows images of proton fluence versus energy and space that were obtained in the direction of the hohlraum pole (LEH) from a series of NIF shots. Two detectors were placed side by side, and protons generated only by shock flash were recorded. The spatial structure of the proton fluence appears to be different not only from shot to shot, but also between the adjacent detector positions in each shot. This indicates that the fluence nonuniformities have unpredictable spatial occurrence, suggesting that the spontaneous fields appearing around the LEHs are random.

However, the measurements do show that one predictable aspect of the fluence nonuniformities in the LEH direction is that they are always present, which means that the spontaneous fields near the LEHs are always present at both shock-flash time and compression burn time. This repeatable temporal occurrence is also seen in related experiments that used proton backlighting methods [28–37] to radiograph hohlraums from the side, where the time-resolved images show that significant deflection of backlighting protons occurred near the LEHs primarily at the times around the fusion burns (shock flash and compression) [31, 33, 37]. The preliminary study has shown that this time coincidence is related to the hohlraum plasma blowoff because the spontaneous fields, primarily generated around the hohlraum wall and stagnated on axis, were subsequently convected with outward plasma flow. The adiabatic expansion of such a flow near the hohlraum LEHs causes plasma to be unstable. The growth of resistive magneto-hydrodynamic instabilities [35, 37] could lead to amplification of the fields near the hohlraum LEHs, resulting in deflection of the fusion protons that are passing through these regions.

3.2. Scale of spatial nonuniformity

As discussed above, figures 5 and 6 show that the proton fluence distributions measured at two adjacent positions in the direction of an LEH during one implosion are different, with no spatial correlation, indicating that the structures of the fields are random. These fluence images taken simultaneously at two positions can therefore be used to estimate the spatial scale of fluence asymmetries. Figure 2 schematically shows the configuration of two detectors installed at the NIF gated-x-ray diagnostics (GXD) holder on the DIM (0, 0). The distance between

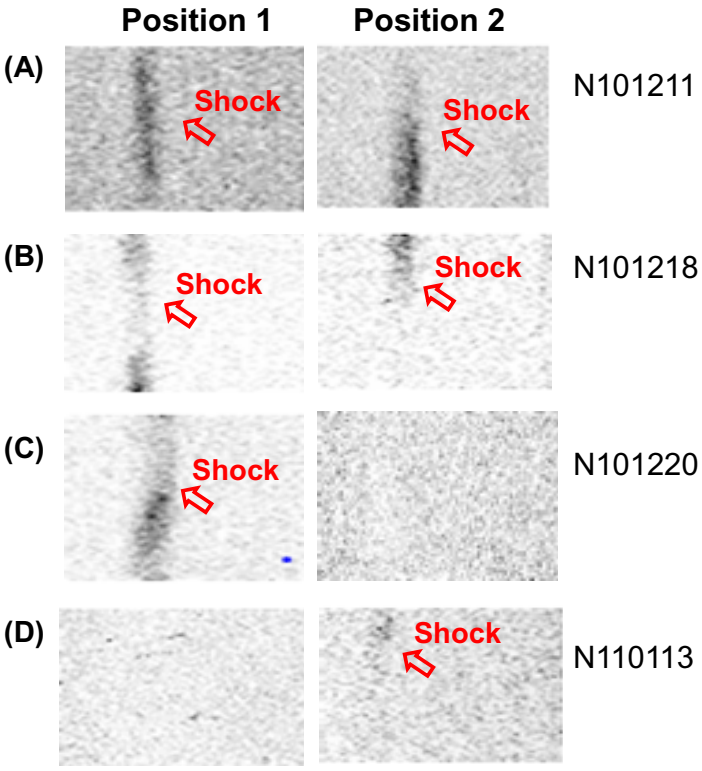

Figure 6. Images of self-emitted proton fluence versus energy and space, measured simultaneously in the direction of the LEH from several NIC shots. Fluence nonuniformities are observed for all shots, and are different for two adjacent detectors in the LEH direction. Proton fluence was focused locally for some observations, for example for the image at Position 1 in (C). The most extreme cases are seen when protons were completely deflected away from the detector plane at Position 2 in (C) or Position 1 in (D). Panel (C) shows that the proton fluence can be completely deflected across the detector plane (Position 2). The random distribution indicates that the spatial occurrence of the proton fluence asymmetry is unpredictable.

detector 1 (Position 1) and detector 2 (Position 2) is about 7 cm (center-to-center), which corresponds to a separation angle $\theta \approx 8^\circ$ and sample plasmas $\sim$1.5 mm apart at the LEH. This number is about 25% of the rough size of the plasma blowoff from an LEH (of the order of the hohlraum diameter). As shown in figures 5 and 6, the largest asymmetry that we have measured is that one detector has signal but another one does not, implying that 1.5 mm can be taken as a characteristic scale of the field asymmetry. Taking this characteristic scale as a wavelength, i.e. $\lambda \sim 1.5$ mm, and assuming the blowoff plasma to have a spherical shape, we find that the mode number of the field nonuniformity is $m = 2\pi r/\lambda \sim 25$, where r is the characteristic radius of the blowoff plasma.

3.3. Undistinguishable field types

Although we have observed proton fluence nonuniformity through the hohlraum LEHs, and have attributed this feature to spontaneous electromagnetic fields, it is very difficult to uniquely

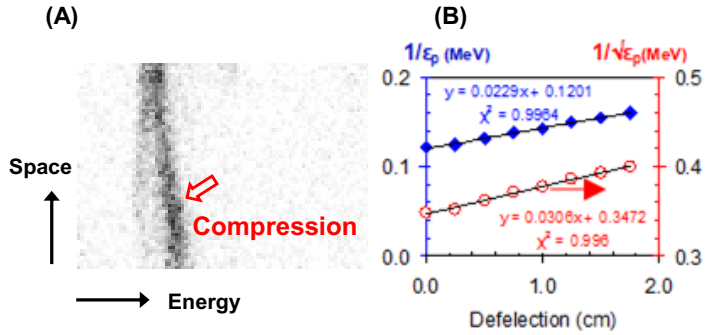

Figure 7. An image of fluence versus energy and space for self-emitted 14.7 MeV D^3He protons from NIC shot N101019, recorded in the direction of the LEH. The proton energy varies continuously with spatial position (A). The deflection distances from the detector plane are plotted against $\varepsilon_p^{-1/2}$ (due to B field) or ε_p^{-1} (due to E field). The good linear fits for both scalings indicate that it is extremely difficult to uniquely determine the field type by using protons with a single energy.

and quantitatively discriminate the field types with the present experimental data. To break the degeneracy among the different possible mechanisms of bending proton trajectories, the Lorentz force law is usually used because the deflection due to either B or E fields will follow different scaling. Specifically, the deflection angle due to B is inversely proportional to the square root of the proton energy ε_p [38],

$$\theta(\boldsymbol{B}, \varepsilon_p) \propto \frac{1}{\sqrt{2m_p\varepsilon_p}} \left| \int \boldsymbol{B} \times \mathrm{d}\ell \right|, \tag{1}$$

while that due to E is inversely proportional to the proton energy [36]

$$\theta(\boldsymbol{E}, \varepsilon_p) \propto \frac{1}{2\varepsilon_p} \left| \int \boldsymbol{E} \times \mathrm{d}\ell \right|. \tag{2}$$

However, in this series of NIC experiments, data were all taken with monoenergetic D^3He protons. With minimum energy loss when they pass through the plasmas, protons with initially a single energy are shown to not have enough dynamic range to resolve the energy information of each individual proton and therefore are not able to uniquely discriminate the different field types. To illustrate this, figure 7(A) shows a spectrally resolved proton image from NIF shot N101019 where the proton deflections were recorded continuously crossing the whole detector plane. The deflections (distances) are plotted against either $\varepsilon_p^{-1/2}$ (due to B field) or ε_p^{-1} (due to E field) in figure 7(B). The measurements are shown to fit well with linear functions, suggesting that the measured deflections in this measurement could be caused by either B or E fields. The range of deflection is apparently too small to resolve the finite difference of individual field energy dependences with a single type of proton. Since the deflections due to collisional scattering in the plasma are too small and have been neglected, breaking the field degeneracy requires using protons with two or more very accurately known initial energies. For example, simultaneously backlighting the hohlraum LEHs with monoenergetic 14.7 MeV D^3He protons

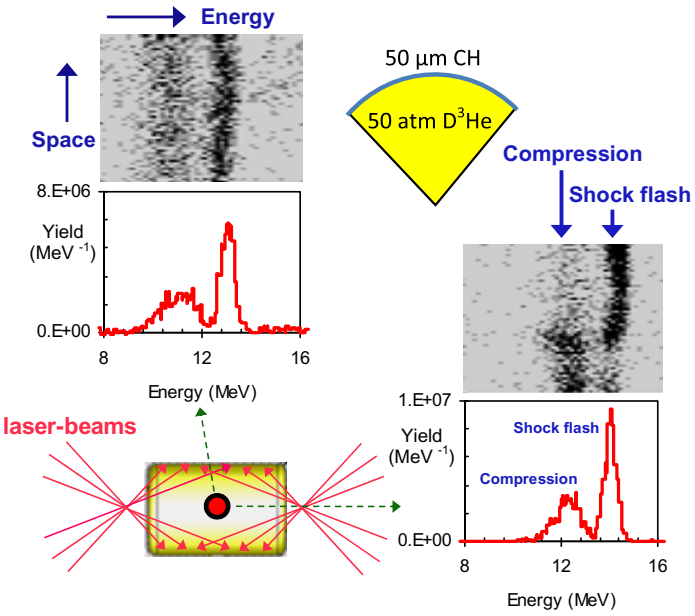

Figure 8. Images of 14.7 MeV proton fluence recorded simultaneously in two different directions relative to the hohlraum in OMEGA shot 54741. The proton yields associated with shock-coalescence burn (the narrow high-energy peak (bang, in image)) and compression burn (the broad low-energy peak (bang)) are clearly separated by energy. The proton fluence in the direction of the LEH is nonuniform at both shock flash and compression burn times, while it is uniform in the equator direction [37].

and 3 MeV DD protons has recently been performed and is expected to provide quantitative information for discriminating B and E fields.

3.4. Estimate of field strengths

Although the field types cannot be uniquely discriminated in this series of experiments, the field strengths can be estimated if we assume that a specific field type is completely dominant. Figure 6 shows that the proton fluence has been either 'uniformly' deflected across the detector plane or focused locally, and sometimes even 'completely' deflected across both detectors (figure 6(D)). These features provide useful information for estimating a lower limit because more deflections could occur beyond what can be measured with the current diagnostic system. Taking $L = 2\,\mathrm{mm}$, $\int \boldsymbol{B} \times \mathrm{d}\boldsymbol{\ell} \sim 2000\,\mathrm{MG}\,\mu\mathrm{m}$ implies that $B \sim 1\,\mathrm{MG}$, while $\int \boldsymbol{E} \times \mathrm{d}\boldsymbol{\ell} \sim 1.5 \times 10^7\,\mathrm{V}$ implies that $E \sim 5\,\mathrm{GV\,m^{-1}}$; these are lower limits of the field strength.

4. Similar observations from OMEGA experiments

The measured fluence nonuniformity of charged fusion products from NIC experiments with ignition scale hohlraums are also observed in experiments at OMEGA with energy-scaled hohlraums, as shown in figure 8. This fact suggests that the underlying physics of such observations is essentially the same. In the OMEGA experiments, the cylindrical, vacuum

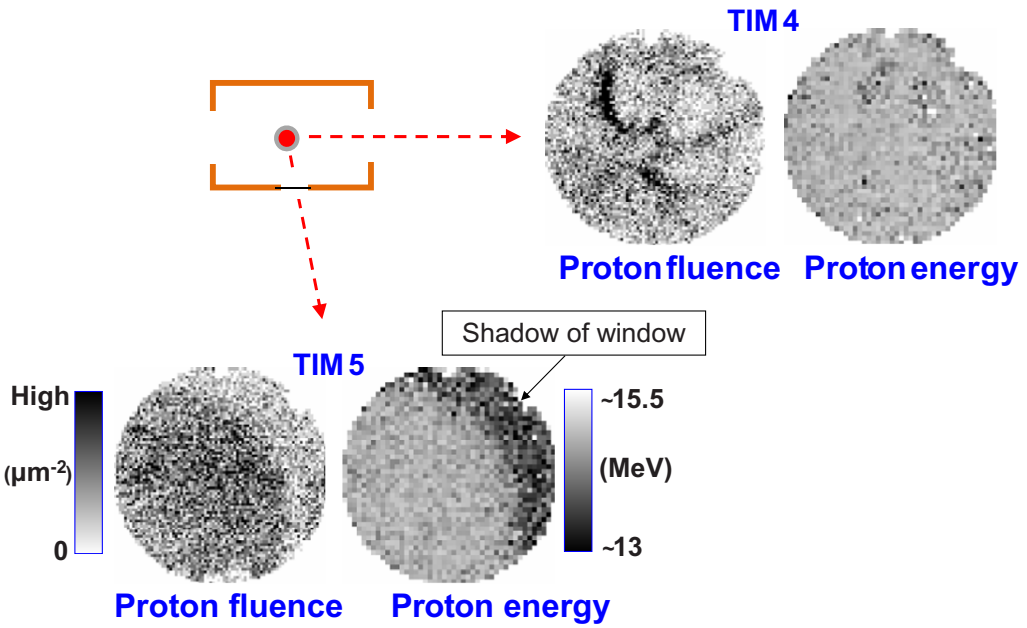

Figure 9. Images showing fluence and mean energy, respectively, of self-emitted D^3He protons as a function of position in detectors viewing the capsule from two different directions in OMEGA shot 54741. Compared with the self-emission image made in the equatorial direction, the one recorded through the LEH shows very nonuniform proton fluence, but it also shows no significant correlated nonuniformities in energy. This suggests that the observed fluence variation has been largely caused by fields near the LEHs and not by proton scattering in the plasma, because Coulomb interactions are always accompanied by energy loss [26].

Au hohlraum was 2.45 mm long with a 1.6 mm diameter and a 0.8 mm diameter LEH. The 647 μm diameter CH capsule had a shell thickness of 48.2 μm and was filled with 50 atm of D^3He (at equal number densities) gas. The hohlraum was driven by 40 beams with total laser energy of 19.7 kJ in a 1 ns square pulse. It is clear in the figure that while the proton fluence in the direction of the equator is spatially uniform, the fluence in the LEH direction shows nonuniformities that are different for the shock flash and compression.

These observed fluence nonuniformities and associated fields were also studied with spectrally resolved images of self-emitted protons from both the hohlraum equator and LEHs, as shown in figure 9. While the proton fluence in the direction of the equator is once again spatially uniform, the fluence in the direction of the LEH is nonuniform with a spatial variation of ~1–2 cm at the detector plane. These measurements are qualitatively consistent with the images shown above.

From all these experimental observations, it is clear that strong fields likely appear in the region near the LEH where the outward-directed axial plasma becomes increasingly resistive after the laser drive ends, leading to the generation, growth and saturation of low-mode-number magneto-instabilities. The data also suggest that the spatial structure and/or the directions of such fields change substantially between the time of shock flash and compression burn. This hypothesis will be experimentally studied in our future work.

5. Summary

In summary, comprehensive spectra and spectrally resolved one-dimensional fluence variations of 14.7 MeV D^3He protons from indirect-drive implosions at the NIF have uniquely demonstrated the existence of strong fields around the laser-entrance holes of ignition-scale hohlraums. Such fields persist even at ~0.5–2.5 ns after the laser has been turned off, generating large deflections and fluence nonuniformities in the hohlraum polar direction. The structure of the fields is unpredictable, and the spatial distribution suggests that the strong fields likely result from the outward flow through the LEH of the on-axis, stagnated plasmas. Data from the current experiments have not been able to uniquely identify the fields as electric or magnetic, but preliminary analysis indicates that the observed charged-particle deflections could be due to either ~1 MG B fields or $\sim 10^9$ V cm^{-1} E fields. Understanding the generation, evolution, interaction and dissipation of such self-generated fields may help to explain a large variety of observed phenomena in indirect-drive ICF experiments, including the large electron temperatures measured in the LEH region, and to validate hydrodynamic models of implosions prior to stagnation in the center of the hohlraum. These experiments provide novel physics insight into the ongoing ignition experiments at the NIF.

Acknowledgments

This work was partially supported by the US DOE and Laboratory for Laser Energetics National Laser User's Facility (DE-FG52-07 NA280 59 and DE-FG03-03SF22691), Lawrence Livermore National Laboratory (B543881 and LD RD-08-ER-062), Laboratory for Laser Energetics (414090-G), Fusion Science Center (412761-G) and General Atomics (DE-AC52-06NA 27279). ABZ is supported by a Stewardship Science Graduate Fellowship (DE-FC52-08NA28752).

References

[1] Nuckolls J *et al* 1972 *Nature* **239** 139
[2] Lindl J D 1999 *Inertial Confinement Fusion* (New York: Springer)
[3] Atzeni A and Meyer-Ter-Vehn J 2004 *Physics of Inertial Fusion* (Oxford: Clarendon)
[4] McCrory R L *et al* 2008 *Phys. Plasmas* **15** 055503
[5] Moses E I *et al* 2005 *Fusion Sci. Technol.* **47** 314
[6] Glenzer S H *et al* 2010 *Science* **327** 1228
[7] Landen O L *et al* 2010 *Phys. Plasmas* **17** 056301
[8] Froula D H *et al* 2010 *Phys. Plasmas* **17** 056302
[9] Meezan N B *et al* 2010 *Phys. Plasmas* **17** 056304
[10] Michel P *et al* 2010 *Phys. Plasmas* **17** 056305
[11] Haan S W *et al* 2011 *Phys. Plasmas* **18** 051001
[12] Edwards M J *et al* 2011 *Phys. Plasmas* **18** 051003
[13] Town R P J *et al* 2011 *Phys. Plasmas* **18** 056302
[14] Hammel B A *et al* 2011 *Phys. Plasmas* **18** 056310
[15] Reagan S P *et al* 2012 *Phys. Plasmas* **19** 056307
[16] Jones O S *et al* 2012 *Phys. Plasmas* **19** 056315
[17] Spears B K *et al* 2012 *Phys. Plasmas* **19** 056316
[18] Callahan D A *et al* 2012 *Phys. Plasmas* **18** 056305

[19] Mackinnon A J *et al* 2012 *Phys. Rev. Lett.* **108** 215005
[20] Robey H F *et al* 2012 *Phys. Rev. Lett.* **108** 215004
[21] Zylstra A B *et al* 2012 *Rev. Sci. Instrum.* **83** 10D901
[22] Soures J M *et al* 1996 *Phys. Plasmas* **3** 2108
[23] Séguin F H *et al* 2003 *Rev. Sci. Instrum.* **74** 975
[24] Séguin F H *et al* 2012 *Rev. Sci. Instrum.* **83** 10D908
[25] Ziegler J F, Biersack J P and Littmark U 1985 *The Stopping and Range of Ions in Solids* (New York: Pergamon)
[26] Li C K *et al* 1993 *Phys. Rev. Lett.* **70** 3059
[27] Séguin F H *et al* 2002 *Phys. Plasmas* **9** 3558
[28] Li C K *et al* 2006 *Phys. Rev. Lett.* **97** 135003
[29] Li C K *et al* 2008 *Phys. Rev. Lett.* **100** 225001
[30] Rygg J R *et al* 2008 *Science* **319** 1223
[31] Li C K *et al* 2009 *Phys. Rev. Lett.* **102** 205001
[32] Petrasso R D *et al* 2003 *Phys. Rev. Lett.* **90** 095002
[33] Li C K *et al* 2012 *Phys. Rev. Lett.* **108** 025001
[34] Li C K *et al* 2007 *Phys. Rev. Lett.* **99** 015001
[35] Li C K *et al* 2009 *Phys. Rev.* E **80** 016407
[36] Li C K *et al* 2002 *Phys. Rev. Lett.* **89** 165002
[37] Li C K *et al* 2010 *Science* **327** 1231
[38] Jackson J D 1975 *Classical Electrodynamics* (New York: Wiley)